

Simultaneous spectrum of Sgr A* and low frequency cut-off

T. An¹, W. M. Goss², J.-H. Zhao³, X. Y. Hong¹, S. Roy⁴, A. P. Rao⁴ and Z.-Q. Shen¹

ABSTRACT

We present a simultaneous spectrum of Sgr A* observed on June 17, 2003. The flux densities of Sgr A* at wavelengths of 90, 26, 23, 20, 17, 6, 3.6, 2, 1.3 and 0.7 cm were measured using the VLA and at 47 cm using the GMRT. On the same date, the SMA and Keck II observed Sgr A* at 0.89 mm and at 3.8 mm, respectively. In agreement with Falcke et al (1998), the spectrum at centimeter wavelengths suggests the presence of a break near $\nu_b \approx 3.6$ cm (8.3 GHz). The spectrum between 0.89 mm and 3.6 cm can be fitted with a power law with a spectral index of $\frac{0.89\text{mm}}{3.6\text{cm}} = 0.43 \pm 0.04$, while the spectrum between 3.6 cm and 47 cm can be described by a flat power law with a spectral index of $\frac{3.6\text{cm}}{47\text{cm}} = 0.11 \pm 0.03$. Sgr A* is measured at 90 cm with a flux density of 0.22 ± 0.06 Jy, suggesting a sharp decrease in flux density at wavelengths longer than 47 cm. The spectrum below 640 MHz ($> 47\text{cm}$) appears to be consistent with free-free absorption by a screen of ionized gas with a cut-off wavelength at $\lambda_c (\nu = 1)$ near 100 cm. However, this cut-off wavelength appears to be three times longer than that of 30 cm (1 GHz) as suggested by Davies et al. (1976) based on observations in 1974 and 1975. Our analysis suggests that the flux density at wavelengths longer than 30 cm could be attenuated and modulated by stellar winds from massive stars in the vicinity of Sgr A*.

Subject headings: Galaxy: center | radio continuum ; galaxies | accretion | black hole physics

¹Shanghai Astronomical Observatory, Chinese Academy of Sciences, Shanghai 200030; an-tao@center.shao.ac.cn

²NRAO-AOC, P.O. Box 0, Socorro, NM 87801; m.goss@ao.nrao.edu

³Harvard-Smithsonian CfA, 60 Garden St, MS 78, Cambridge, MA 02138; jzhao@cfa.harvard.edu

⁴National Center for Radio Astrophysics (TIFR), Pune University Campus, Post Bag No. 3, Ganeshkhind, Pune 411 007, India

1. INTRODUCTION

Soon after the discovery of the compact radio source Sagittarius A* (Sgr A*) at the Galactic center (GC) (Balick & Brown 1974), Davies et al. (1976, hereafter DWB) observed Sgr A* at 0.408, 0.960 and 1.660 GHz. As a result, Sgr A* was only detected at the two higher frequencies. The measurements showed a low frequency cutoff at ~ 1.3 GHz in the spectrum of Sgr A* and the authors suggested that the decrease in the flux density below 1 GHz was due to free-free absorption by ionized gas in the Sgr A West. Based on the earlier VLA images of the Galactic center region, Pedlar et al. (1989) reported a non-detection of Sgr A* with an upper limit < 0.1 Jy at 330 MHz in consistent with the free-free absorption model suggested by DWB. However, the spectrum at frequencies lower than 1 GHz is now open to question due to the detection of Sgr A* at 620 MHz with the GMRT (Roy & Rao 2004). This detection of $0.5 - 0.1$ Jy at 620 MHz may be in conflict with the conclusion of DWB in 1976. In a recent paper, Nord et al. (2004) reported a flux density of $0.33 - 0.12$ Jy at 330 MHz from VLA A array observations performed in 1996 and 1998 with a higher angular resolution of $6.8'' - 10.9''$.

Sgr A* is now believed to be associated with a supermassive black hole (SMBH) with a mass of $\sim 4 \times 10^6 M_{\odot}$ (Schodel et al. 2002; Gez et al. 2005). This unique source can be studied in detail due to the proximity to the Sun ($1''$ corresponds to 0.04 pc at a distance of 8 kpc, Reid et al. 1999); thus it is possible to evaluate astrophysical processes near SMBHs. A number of models have been proposed to explain the observations from the vicinity of Sgr A* at radio, submillimeter, near-IR and X-ray wavelengths. In general, the models suggest low efficiency radiative accretion flows or outflows in order to explain the weak nature of Sgr A* (Narayan & Yi 1994; Falcke & Marko 2000; Melia, Liu, & Coker 2001; Yuan, Marko, & Falcke 2002; Liu, Petrosian, & Melia 2004). In a recent paper, Loeb (2004) proposed that stellar wind streams from young massive stars close to Sgr A* might also play an important role in fuelling Sgr A* and therefore caused the variations in flux density at millimeter/submillimeter wavelengths. These models are sensitive to the observed spectrum of Sgr A*. Simultaneous multi-wavelength observations could provide important constraints to current accretion or outflow theories. In particular, if stellar winds are indeed responsible for the flux density variations at millimeter/submillimeters, a cutoff at low radio frequencies might be sensitive to the change in stellar wind flux near Sgr A*.

We observed Sgr A* with the VLA at wavelengths of 90, 26, 23, 20, 17, 6, 3.6, 2, 1.3 and 0.7 cm on June 17, 2003 (UT). At the same epoch, the Giant Metrewave Radio Telescope (GMRT) also observed Sgr A* at 47 cm (640 MHz). The VLA and GMRT observations were carried out in order to determine the lower frequency cutoff in the spectrum of Sgr A*. Fortunately, both the Submillimeter Array (SMA hereafter, Ho, Moran & Lo 2004) and

Keck II also observed Sgr A* at 0.89 mm and 3.8 mm, respectively, on June 17, 2003. In this letter, we present new results from the quasi-simultaneous spectrum of Sgr A* observed on June 17, 2003.

2. OBSERVATIONS AND DATA REDUCTION

Sgr A* was observed at multiple wavelengths with four telescopes on June 17, 2003. The observations with the VLA were performed in the A configuration at wavelengths ranging from 90 cm up to 7 mm. Table 1 summarizes the observations: observing band (λ), frequency (ν), bandwidth ($\Delta\nu$) in each IF, on-source time (t) and the resolution of the array. The observations at 90 cm and 20 cm were carried out in spectral-line modes in order to reject radio frequency interference and minimize the bandwidth smearing effect.

The strong sources 3C 286 (at 0.7, 1.3 and 2 cm) and 3C 48 (at 3.6, 6, 17, 20, 23, 26 and 90 cm) were observed as primary flux density calibrators at the beginning or the end of the observing runs. A few nearby QSOs were observed and interleaved with the observations of Sgr A* in order to determine the complex gains. The data reduction of the VLA observations was carried out using the Astronomical Image Processing System (AIPS) of the National Radio Astronomy Observatory (NRAO). The VLA data reduction was carried out following the standard procedure in AIPS. We also performed several iterations of phase self-calibrations to correct for the residual phase errors. The final continuum image at 90 cm was made with the maximum-entropy task VTESS in AIPS with a beam size of $14.5'' \times 5.7''$ at PA of 24.4° .

The observation at 47 cm (640 MHz) was carried out with the GMRT from 20:30 to 22:30 (UT). The data were calibrated with the GMRT calibration procedure and the images were made in the AIPS with a uv range of 10-50 k to minimize background contamination. A flux density of 0.45 ± 0.10 Jy at 640 MHz was determined after the background was subtracted using JMFIT.

3. DATA ANALYSIS AND RESULTS

3.1. Flux density measurement of Sgr A* at 90 cm

Figure 1 shows a pseudo-color image of Sgr A* at 90 cm. In order to compare our results with those obtained by Nord et al. (2004) at the same wavelength, we restored the final image using a synthesized beam similar to values used by Nord et al. (2004), i.e., $10.9'' \times 6.8''$

(PA = 10°). The r.m.s. noise in the image is 12 mJy/beam estimated from an off-source region. A r.m.s. noise about 4 mJy/beam is obtained by Nord et al. (2004) with a longer on-source time. The supernova Sgr A East dominates the total flux density at 90 cm. The emission from the Sgr A East shows an asymmetric structure: the emission from the shell to the east appears to be significantly brighter than the emission to the west, as pointed out earlier by Pedlar et al. (1989). The red cross at the image center marks the position of Sgr A* (Rogers et al. 1994) and its expected scattering size at 90 cm, i.e., 11⁰⁰ 6⁰⁰ at PA = 80° (Lo et al. 1998). An excess in flux density is observed at the expected location of Sgr A*. The region surrounding Sgr A* is significantly absorbed by the ionized gas in the Sgr A West except for the extended emission south to Sgr A*. We made two slices along the major (PA = 80°) and minor (PA = 10°) axes of the expected scattering shape to determine the flux density (Figure 2). Gaussian profiles were fitted to each of the slices after subtracting the diffuse emission from the background; an apparent size of (16:0⁰⁰ 1:3⁰⁰) (15:3⁰⁰ 2:5⁰⁰) was determined. The r.m.s. errors of the positions in the image ($\frac{\text{beam size}}{2 \text{ SNR}}$), together with the errors in gaussian fitting and the uncertainties due to map noise, are taken as the total uncertainty of measured source sizes. The r.m.s. error in the image along the minor axis is larger than that along the major axis due to confusion from Sgr A East to the south of Sgr A*. The inferred intrinsic size of Sgr A* at 90 cm is (14:4⁰⁰ 1:4⁰⁰) (10:7⁰⁰ 2:4⁰⁰) after deconvolution with the synthesized beam. A position angle with 1σ error of 95 ± 25° has been estimated. The fitted peak flux density is 65 ± 16 mJy/beam and a total flux density of 220 ± 60 mJy is determined. The uncertainty of the total flux density includes both the calibration errors and gaussian fitting errors. The properties of the source at 90 cm agree with the determinations of Nord et al. (2004) within one sigma.

3.2. Simultaneous Spectrum at Radio Wavelengths

The flux densities of Sgr A* at higher frequencies were measured in images made from the calibrated data. Either a point-source model or an elliptical Gaussian model was used to fit the data. At 20 cm, Sgr A* is slightly resolved; thus a two-dimension elliptical Gaussian function was used. At 6 and 3.6 cm, the emission from the H II region in Sgr A West is resolved out with baselines longer than 80 kλ and the flux density from Sgr A* is then dominant. The free-free components in the Sgr A West in the vicinity of Sgr A* at 2, 1.3 and 0.7 cm are resolved out by the configuration of the VLA. Sgr A* dominates the visibilities at these three wavelengths and can be described by a point source at the phase center. To compare with the measurements from the image domain, we have also determined the flux density at each wavelength in the uv domain. The difference in flux densities derived between the two procedures is consistent with the uncertainty (σ_M) in the measurements

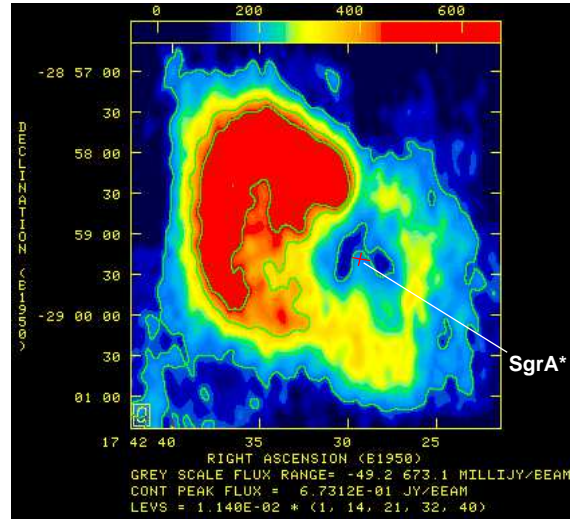


Fig. 1. | Pseudo-color/contour image of Sgr A* at 90 cm. Contours: 11:4 (1;14;21;32;40) m Jy/beam. The image is restored with a synthesized beam of $10.8^{00} \times 6.9^{00}$ (PA = -10). The red cross in the image center marks the expected scattering size and position of Sgr A* at 90 cm, i.e., $11^{00} \times 6^{00}$ at PA .80 (Rogers et al. 1994; Lo et al. 1998).

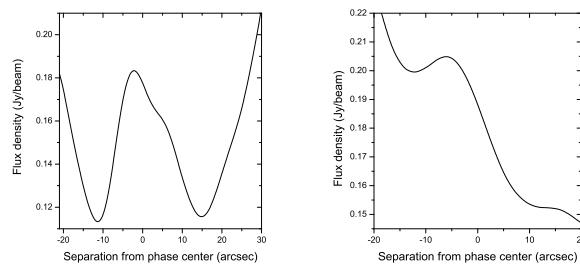


Fig. 2. | Left: The radio intensity at 90 cm cut along expected major axis, (PA = 80) in Fig. 1. The slice is centered at $17^h 42^m 29^s.4, -28 59^0 18^{00}.1$ (J2000) with a resolution of 6.9^{00} . East is toward the left. Right: Slice along the expected minor axis of Sgr A* (PA = -10) with a resolution of 10.8^{00} . South is toward the left.

due to the bias errors in the visibilities or the r.m.s. in the images. On the other hand, the calibration uncertainty (σ_c) appears to be dominated by the uncertainty in the flux density scale. Thus, the inferred 1σ errors are the quadrature addition of the two terms $\sigma_p \sqrt{\frac{2}{M} + \frac{2}{C}}$. The measurements of flux densities at 2, 1.3 and 0.7 cm are consistent with the values derived from the monitoring program (Hermstein et al. 2004). Table 2 presents the measured flux density and 1σ uncertainty at each wavelength.

Figure 3 shows the quasi-simultaneous spectrum of Sgr A* at wavelengths in the range between 90 cm and 3.8 mm on June 17, 2003. The measurements are from the observations with the VLA from 90 to 0.7 cm (solid circle), with the GMRT at 47 cm (diamond), with the SMA at 0.89 mm (triangle; Zhao et al. 2005) and the Keck II observations at 3.8 mm (square; Ghez et al. 2004). A rising spectrum appears to extend from 15 GHz up to somewhere at millimeter/submillimeter wavelengths although the exact peak frequency remains uncertain. For wavelengths from the shorter centimeter to millimeter wavelengths, the rising spectrum can be described by a power law (S/ν^α) with $\frac{0.89\text{mm}}{3.6\text{cm}} = 0.43 \pm 0.04$ (solid line in Figure 3). A spectral index $\frac{3.8\text{mm}}{0.89\text{mm}} = 1.13^{+0.06}_{-0.08}$ is also inferred from the flux densities at 0.89 mm and 3.8 mm assuming a straight power law spectrum. A break near 3.6 cm (8.3 GHz) is seen in the spectrum. The power law fitting suggests that the break wavelength ν_b ranges between 2.8 and 4.2 cm. The spectrum between 3.6 and 47 cm is flat with a spectral index $\frac{3.6\text{cm}}{47\text{cm}} = 0.11 \pm 0.03$ based on the least squares fit (dashed line in Figure 3). The difference in spectral indices between the two parts of the spectrum is $\frac{3.6\text{cm}}{0.89\text{mm}} - \frac{47\text{cm}}{3.6\text{cm}} = 0.32 \pm 0.05$, suggesting a significant break at $3.6^{+0.6}_{-0.8}$ cm on June 17, 2003.

A break in the cm-band spectrum of Sgr A* in a range between 3.5 and 2.0 cm has been observed previously (Zylka et al. 1992; Serabyn et al. 1997; Falcke et al. 1998; Zhao et al. 2003). An excess in flux density towards shorter wavelengths in the spectrum of Sgr A* might be associated with activities in the inner region of the accretion disk or jet nozzle (reviewed by Melia & Falcke 2001). In addition, the spectral index at short centimeter/millimeter wavelengths is found to be correlated with the radio flux density (Hermstein et al. 2004). In comparison with the radio light curves, the larger spectral index at frequencies higher than the break frequency 8.3 GHz on June 17, 2003 is consistent with Sgr A* undergoing a large radio outburst. The VLA monitoring campaign (Hermstein et al. 2004) did show that Sgr A* was in an outburst stage at 7 mm around the epoch of June 16, 2003, and the outburst apparently peaked near the epoch of July 17, 2003. In fact, the flux density at 7 mm on July 17, 2003 was measured at the highest outburst during the monitoring period between June 21, 2000 and October 16, 2003 (Hermstein et al. 2004). Therefore, the break in the spectrum of Sgr A* at a short centimeter could be a signature of synchrotron self-absorption (SSA) of a relatively strong radio outburst (Kellermann & Pauliny-Toth 1969) as was proposed to explain for the 2002-10-03 X-ray event and the corresponding radio outburst (Zhao et al.

2004).

At 90 cm, the measured flux density of 0.22 ± 0.06 Jy is far below the inferred value 0.49 Jy, extrapolated from the power law fitting $S \propto \nu^{-0.11 \pm 0.03}$. The significant decrease ($>4\sigma$) suggests that the spectrum could have a cutoff at wavelengths longer than 47 cm.

4. Discussion

The earlier measurements of Sgr A* made by Davies et al. (1976) showed a low-frequency cutoff in the range of 1–3 GHz in the spectrum. The Jodrell Bank flux densities of 0.26 ± 0.03 Jy at 0.960 GHz and 0.56 ± 0.06 Jy at 1.66 GHz have been corrected for resolutions of the interferometer and angular diameters of Sgr A*. We note that the angular diameters measured with the Jodrell Bank, $1.5'' \pm 0.3''$ at 0.96 GHz and $0.5'' \pm 0.1''$ at 1.66 GHz, are consistent (within 2 σ of the quoted errors) with the values extrapolated from the relationship between the geometrical mean of the angular size and the observing wavelength (Lo et al. 1998; Doeleman et al. 2001; Bower et al. 2004). For an angular size of $1.5''$ (0.96 GHz), Sgr A* is dominant with baseline ranges from 34 to 75 k λ ; and for an angular size of $0.5''$ (1.66 GHz), Sgr A* is dominant with baseline ranges of 60–132 k λ . The errors in flux densities at these two frequencies (10 percent) are consistent with those estimated in our observations. A ratio of $S_{1.66\text{GHz}}/S_{0.96\text{GHz}} = 2.2 \pm 0.3$ (based on the observations during 1974 and 1975) suggests a significant decrease in the flux density at the lower frequency. However, the 408 MHz upper limit measured by DWB with a single baseline should be taken carefully because of the interference between components in the complex region in Sgr A West, surrounding the largely broadened Sgr A* at 408 MHz (e.g. Roy & Rao 2004).

In Figure 4, we compare the low frequency (from 90 to 3.6 cm) spectrum measured at epochs 1975 (open circle, Davies et al. 1976) and 2003 (solid square, present paper). The upper limit at 408 MHz in 1975 has been excluded both in the plot and in the least squares fit. The spectra at both epochs can be fitted with a model of a slowly rising power law spectrum ($S \propto \nu^{-\alpha}$) together with a free-free absorption screen (τ_{ff}) between Sgr A* and the observers, as has been proposed by Davies et al. (1976). If the flux density at 0.960 GHz measured by DWB 28 years ago is reliable, the comparison of least squares fits to the 1976 and 2003 data suggests a significant change in the spectrum of Sgr A* at frequencies below 1 GHz in the past 28 years.

If the free-free absorption model was correct, the variation in the low frequency spectrum would suggest that the column density of the free-free absorbing screen must have changed significantly over the past 28 years. Starting from DWB's free-free absorption model ($S \propto$

$S_0 e^{-\tau_{ff}}$), the quantitative change in the column density of the ionized gas in front of Sgr A* can be assessed. The solid and dashed lines in Figure 4 represent the free-free model fit to the 2003 data and the 1975 data, respectively. At the higher frequencies, the data observed at both epochs can be fitted with a power-law spectrum $S \propto \nu^{-0.074-0.022\nu}$ along with an exponential cutoff at the lower frequencies owing to free-free absorption. The comparison of model fits and observations at these two epochs suggests that the free-free opacity (τ_{ff}) in front of Sgr A* must have decreased by a factor of nine (i.e., the critical cutoff frequency $\nu_c(\tau_{ff} = 1)$ in free-free absorption has decreased from 1 GHz to 300 MHz in the past 28 years). Assuming the electron temperature of the ionized gas remains constant, the inferred decrease in τ_{ff} must correspond to a decrease by a factor of nine in emission measure $EM = \int n_e^2 dl$. Such a large variation in EM is plausible in a small region near Sgr A*, perhaps within the Bondi accretion radius R_{acc} of 0.06 pc (Bagano et al. 2003). Then, the amount of the change in the cutoff frequency ν_c implies that the mean electron density ρ_p $EM = R_{acc}$ within the Bondi accretion radius or the electron column density in front of Sgr A* has decreased by a factor of three in the past 28 years. Therefore the Bondi accretion rate in Sgr A*, \dot{M}_B / n_e , or the accretion rate determined from other models (e.g., ADAF, CDAF and ADIOS) is expected to drop by a factor of three in past 28 years.

The stellar wind streams from the orbiting massive stars around Sgr A* within the central $1''$ (0.04 pc) could modulate the flux density at low radio frequencies from Sgr A* on a timescale of ten years (Loeb 2004). In addition, the flux of stellar winds near Sgr A* could be modulated by orbit motions of the stars. Here we consider two types of stellar winds: (I) a stellar wind is isotropically ($n_e \propto r^{-2}$) and (II) a stellar wind stream forms into a one-dimensional flow under the gravitation of the SMBH ($n_e \propto r^{-1}$). Using S0-2 (Ghez et al. 2005) as an example, the orbit period is about 15 years and the ratio of distance between pericenter and apocenter is about 1:15. The stellar wind flux at pericenter in case I is 200 times that at apocenter; in case II the contrast in stellar wind flux between pericenter and apocenter is 15:1. The ratio of three in electron column density between 1975 and 2003 inferred from the low frequency cutoff variation is much smaller than the maximum contrast of the stellar wind flux in both cases. Considering the collective effect of a number of orbiting stars in the vicinity of Sgr A*, the inferred change in electron column density in a timescale of 28 years is consistent with the stellar wind model. The low frequency cutoff in the radiation spectrum of Sgr A* and the change of the cutoff frequency could be explained by the attenuation owing to varying stellar wind flux from the central star cluster at the Galactic center.

5. Summary

We have constructed the spectrum of Sgr A* on the date of June 17, 2003, over the wavelength range of 3.8 m to 90 cm. We have used data from the GMRT and the VLA, and made use of additional data from the SMA and Keck II. These simultaneous observations confirmed the previous detection of a break wavelength near 3.6 cm. Sgr A* was detected at 90 cm, supporting a recent detection at the same wavelength. The flux density of Sgr A* at 90 cm showed a significant decrease in comparison with that at 47 cm, showing a low-frequency cutoff near 100 cm. Free-free absorption could be responsible for the low-frequency cutoff. The comparison between 1975 data and 2003 data suggested that the free-free opacity in front of Sgr A* has decreased by a factor of nine in past 28 years. Our analysis is consistent with a stellar wind model in which the flux density at wavelengths longer than 30 cm is likely modulated by the stellar wind flux from massive stars in the vicinity of Sgr A*.

The research is supported in part from the National Science Foundation of P.R. China (10328306, 10333020). Tan would like to thank Heino Falcke for valuable comments. The VLA is operated by the National Radio Astronomy Observatory (NRAO). The NRAO is a facility of the National Science Foundation operated under cooperative agreement by Associated Universities, Inc. This research has made use of NASA's Astrophysics Data System (ADS).

REFERENCES

- Balick, B., & Brown, R.L. 1974, *ApJ*, 194, 265
- Bagano, F.K., Mameda, Y., & Morris, M. et al. 2003, *ApJ*, 591, 891
- Bower, G.C., Falcke, H., Herrnstein, R.M., Zhao J.-H., Goss, W.M., Backer, D.C. 2004, *Sci*, 304, 704
- Davies, R.D., Walsh, D., & Booth, R.S. 1976, *MNRAS*, 177, 319
- Doelman, S. et al. 2001, *AJ*, 121, 2610
- Falcke, H., Goss, W.M., Matsuo, H., Teuben, P., Zhao, J.-H., Zylka, R. 1998, *ApJ*, 499, 731
- Falcke, H., & Marko, S. 2000, *A&A*, 362, 113
- Ghez, A.M., Wright, S.A., Matthews, K., et al. 2004, *ApJ*, 601, L159

- Ghez, A M ., Salim , S., Hornstein S D ., et al. 2005, ApJ, 620, 744
- Hornstein, R M ., Zhao, J.-H ., Bower, G C . Goss, W M . 2004, AJ, 127, 3399
- Ho, P.T.P ., Moran, J M ., & Lo, K.Y . 2004, ApJ, 616, L1
- Kellermann, K I., & Pauliny-Toth, I.I.K ., 1969, ApJ, 155, L71
- Liu, S M ., Petrosian, V ., & Melia, F . 2004, ApJ, 611, L101
- Lo, K.Y ., Shen, Z.-Q ., Zhao, J.-H ., Ho, P.T.P . 1998, ApJ, 508, L61
- Lobe, A . 2004, MNRAS, 350, 725
- Melia, F ., Liu S.M ., & Coker, R . 2001, ApJ, 553, 146
- Miyazaki, A ., Tsutsumi, T ., Tsuboi, M . 2004, ApJ, 611, L97
- Narayan, R ., & Yi, I. 1994, ApJ, 428, L13
- Nord, M E ., Lazio, T J.W ., Kassim , N E ., Goss, W M ., & Duric, N . 2004, ApJ, 601, L51
- Pedlar, A ., Anantharamaiah, K R ., & Ekers, R D ., et al. 1989, ApJ, 342, 769
- Reid, M J., Readhead, A C.S., Vermeulen, R C., Treuhaft, R N . 1999, ApJ, 524, 816
- Rogers, A E.E ., Doelman S., Wright M C H ., et al. 1994, ApJ, 434, L59
- Roy, S., & Rao, A P . 2004, MNRAS, 349, L25
- Schodel, R ., Ott, T ., Genzel, R ., et al. Nature, 419, 694
- Serabyn, E ., Carlstrom , J., Lay, O . et al. 1997, ApJ, 490, L77
- Yuan, F ., Marko , S., & Falcke, H . 2002, A & A , 383, 854
- Zhao, J.-H ., Bower, G C ., & Goss, W M . 2001, ApJ, 547, L29
- Zhao, J.-H ., Young, K . H ., Hornstein, R M ., et al. 2003, ApJ, 586, L29
- Zhao, J.-H ., Hornstein, R M ., Bower, G C ., Goss, W M ., Liu, S M . 2004, ApJ, 603, L85
- Zhao, J.-H ., et al. 2005, in preparation
- Zylka, R ., Mezger, P G ., Lesch, H . 1992, A & A , 261, 119

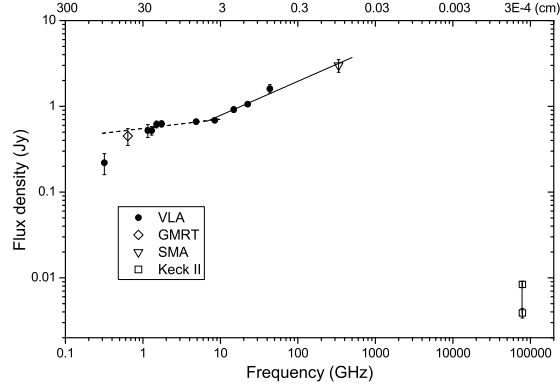


Fig. 3. | A simultaneous spectrum of Sgr A* from 90 cm to 3.8 m on epoch 2003-06-17. solid circle: VLA; diamond: GMRT; triangle: SMA (Zhao et al. 2005); square: Keck II (Ghez et al. 2004).

Table 1: OBSERVATIONAL LOGS

(GHz)	(MHz)	t(min)	Maj(⁰)	Min(⁰),PA(°)
(1)	(2)	(3)	(4)	
0.303,0.332	3.125	29	14.5	5.7, 24.4
0.640	7.5	85	8.6	4.3, 27
1.16,1.30,1.50,1.74	12.5	56	2.23	1.08,13.4
4.835,4.885	50	11	1.00	0.47, 27:7
8.435,8.485	50	11	0.63	0.50, 32:2
14.915,14.965	50	11	0.31	0.13, 25:0
22.435,22.485	50	29	0.19	0.14,25.3
43.315,43.365	50	32	0.17	0.14,34.1

Note : (1) central frequency in each IFs; (2) bandwidth of IFs; (3) on-source time; (4) restored beam .

Table 2: THE RESULTS OF POWER SPECTRAL FITTING FOR SGR A*

(GHz)	0.318	0.640	1.155	1.300	1.500	1.740	4.86	8.46	14.94	22.46	43.34
S (Jy)	0.22	0.45	0.522	0.522	0.617	0.625	0.663	0.687	0.918	1.060	1.607
(Jy)	0.06	0.10	0.089	0.059	0.056	0.050	0.036	0.031	0.064	0.060	0.180
c (%)	9.9		3.4	3.9	5.3	5.2	4.0	3.9	6.9	5.3	10.9
M (%)	25.0		17.0	10.7	7.4	5.6	3.6	2.3	1.2	1.9	0.9

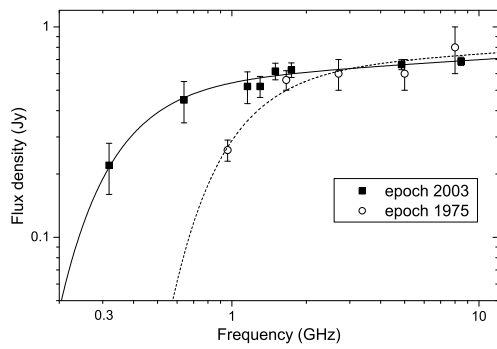


Fig. 4. Comparison of low frequency spectrum s of Sgr A * between epochs 1975 (solid square) and 2003 (open circle). The dashed and solid lines represent free-free ts to the spectrum at epochs 1975 and 2003, respectively.